

UVES radial velocity accuracy from asteroid observations

I. Implications for the fine structure constant variability[★]

P. Molaro¹, S. A. Levshakov², S. Monai¹, M. Centurión¹, P. Bonifacio^{1,3}, S. D’Odorico⁴, and L. Monaco⁵

¹ INAF-Osservatorio Astronomico di Trieste. Via G.B. Tiepolo 11 I-34143, Trieste, Italy

² Department of Theoretical Astrophysics, Ioffe Physico-Technical Institute, Polytekhnicheskaya Str. 26, 194021 St. Petersburg, Russian Federation

³ CIFIST, Marie Curie Excellence Team and GEPI, Observatoire de Paris, CNRS, Université Paris Diderot; Place Jules Janssen 92190, Meudon, France; Observatoire de Paris 61, CNRS avenue de l’Observatoire, 75014 Paris, France

⁴ European Southern Observatory, Karl-Schwarzschild-Strasse 2, D-85748 Garching bei München, Germany

⁵ European Southern Observatory, Alonso de Crdova 3107, Casilla 19001, Vitacura, Santiago, Chile

Received October ..., 2007; accepted ...

ABSTRACT

Context. High resolution observations of the asteroids Iris and Juno have been performed by means of the UVES spectrograph at the ESO VLT to obtain the effective accuracy of the spectrograph’s radial velocity. The knowledge of this quantity has important bearings on studies searching for a variability of the fine structure constant carried on with this instrument.

Aims. Asteroids provide a precise radial velocity reference at the level of 1 m s^{-1} which allows instrumental calibration and the recognition of small instrumental drifts and calibration systematics. In particular, radial velocity drifts due to non uniform slit illumination and slit optical misalignment in the two UVES spectrograph arms can be investigated.

Methods. The position of the solar spectrum reflected by the asteroids are compared with the solar wavelength positions or with that of asteroid observations at other epochs or with the twilight to asses UVES instrumental accuracy .

Results. Radial velocities offsets in the range $\approx 10\text{--}50 \text{ m s}^{-1}$ are generally observed likely due to a non uniform slit illumination. However, no radial velocity patterns with wavelength are detected and the two UVES arms provide consistent radial velocities. These results suggest that the detected $\Delta\alpha/\alpha$ variability by Levshakov et al. (2007) deduced from a drift of $-180 \pm 85 \text{ m s}^{-1}$ at $z_{\text{abs}}=1.84$, between two sets of Fe II lines falling in the two UVES arms may be real or induced by other kinds of systematics than those investigated here. The proposed technique allows real time quality check of the spectrograph and should be followed for very accurate measurements.

Key words. radial velocities – fundamental physics – qso – asteroids

1. Introduction

Radial velocity precision is required in several fields of astronomical research ranging from the detection of exoplanets to the study of the variability of the fundamental physical constants. To reveal the presence of an orbiting planet dedicated spectrographs have been manufactured to achieve the best accuracy in the radial velocity. With HARPS at the 3.6 m telescope a relative precision of 1 m s^{-1} or higher has been achieved when the full optical stellar spectrum of a solar type star is recorded and compared in different epochs. Search for a possible variability of the fine structure constant, $\Delta\alpha/\alpha = (\alpha_z - \alpha)/\alpha$, at a redshift z , is currently carried out by measuring line shifts between different lines of absorbers observed in spectra of distant quasars which show different sensitivities to α (Webb et al. 1999, Dzuba et al. 2002). QSOs are rather faint and require large telescopes such as VLT or Keck combined with the high resolution spec-

trographs, UVES and HIRES respectively. Murphy et al. (2004) claim that $\Delta\alpha/\alpha = -5.7 \pm 1.1 \text{ ppm}$ (ppm stands for parts per million, 10^{-6}) by averaging over 143 absorption systems detected in HIRES/Keck telescope spectra of QSOs in a redshift range $0.2 < z < 4.2$ implying that in the past the fine structure constant was smaller. On the other hand no variability has been measured by a different group at the VLT with UVES adopting similar techniques (Quast et al. 2004, Chand et al. 2004, Levshakov et al. 2005, 2006; but see also Murphy et al. 2006 and Srianand et al. 2007). More recently Levshakov et al. (2007) measured a radial velocity difference of $-180 \pm 85 \text{ m s}^{-1}$ between Fe II transitions falling in the two different arms of the UVES providing evidence for a variation in the fine structure constant $\Delta\alpha/\alpha = 5.4 \pm 2.5 \text{ ppm}$, with the fine structure constant being larger in the past at odds with what found by Murphy et al. (2004). Given the importance of these results for fundamental physics a thorough investigation of systematic errors to rule out possible instrumental shifts which may occur during UVES observations is rather crucial.

Spectroscopic observations are generally calibrated in wavelength by means of standard calibration lamps, namely the ThAr

Send offprint requests to: P. Molaro

[★] Based on observations performed at the VLT Kueyen telescope (ESO, Paranal, Chile).

lamps. However, to achieve a $\Delta\alpha/\alpha$ of 1 ppm a precision of 30 m s^{-1} in the radial velocity of the most sensitive lines is required challenging the spectrograph precision. Small instrumental effects could be present since the light paths of calibration and stellar beams are different when entering the spectrograph slits. Instrumental flexures, temperatures and atmospheric pressure instability can produce small radial velocity shifts between calibration and science observations. Temperature and pressure variations as small as $\Delta T = 0.3 \text{ K}$ or a $\Delta P = 1 \text{ mbar}$ produce a drift of $\approx 50 \text{ m s}^{-1}$ (Kaufer et al. 2004). These effects can be minimized by taking ThAr lamps immediately before or after the science exposures if ambient conditions do not change in the meantime. However, an uneven illumination of the slit may cause spectral shifts and therefore errors in the measurements of radial velocities. This problem is particularly acute in the case of UVES observations with the dichroic mode where the light enters two distinct slits of the two arm spectrograph. Possible effects of different illumination of the two slits of the blue and red arms of UVES are unknown.

To probe small possible instrumental effects in UVES, we observed the solar spectrum reflected by asteroids which are sources with radial velocities known at the m s^{-1} level. This accuracy is not required by the majority of the observations but is crucial for the investigation of variability of the fine structure constant. The presence of a variability of fundamental dimensionless constants would be a discovery of the utmost importance in theoretical physics with far reaching implications (Copeland et al. 2006, Avelino et al. 2006, Martins 2006, Fujii 2007).

2. Observations and data analysis

Observations of two asteroids Iris and Juno together with observations of the sunlight at twilight have been collected at the VLT by means of the UVES spectrograph between December 2006 and January 2007 as reported in Table 1. UVES is a two-arm crossdispersed echelle spectrograph with the possibility to use dichroic beam splitters and to record most of the optical spectrum with one observation (Kaufer et al. 2004). The observations have been taken with the dichroic mode, the ESO DIC1, allowing simultaneous observations of the blue and red arms. This dichroic has a cross-over wavelength at 450 nm and the central wavelengths were set at 390 nm for the blue and at 580 nm for the red arms respectively, allowing a full spectral range from 350 nm up to 680 nm.

We used a 0.5 arcsec slit providing a resolving power of about $\frac{\lambda}{\delta\lambda} \approx 80,000$ which is the maximum resolution that can be reached with still adequate sampling of the PSF. It is relevant to note that the target is centered on one of the spectrograph slits, the red slit in our case, while there is no way to check the optical centering on the blue arm slit, directly. The slits were aligned with the parallactic angle in order not to miss light due to atmospheric diffraction. The two UVES arms are equipped with CCD detectors, one single chip in the blue arm and a mosaic of two chips in the red arm. The blue CCD is a $2\text{K} \times 4\text{K}$, 15μ pixel size thinned EEV CCD-44 while the red CCD mosaic is made of an EEV chip of the same type and a MIT/LL CCID-20 chip for the redder part of the spectral range. Each arm has two crossdisperser gratings working in the first spectral order.

Asteroids are apparently fast moving objects and the geocentric radial velocity changes by about 1 m s^{-1} in about 4 minutes typically, thus limiting the maximum exposure time also with the largest telescopes. At the epoch Iris and Juno were of 8 and 10.6

mag, respectively, and we kept the exposures at 300 and 900 s achieving a signal-to-noise between 100–200.

The observations were bracketed by ThAr standard calibration lamps. Calibration and science observations were carried on in the attached mode to avoid the automatic resetting of the spectrograph position, implemented by ESO on 26 Dec 2001, to compensate thermal drifts in the dispersion direction between daytime calibration frames and science observations. The automatic resetting of the instrument allows calibration frames to be taken in daytime with an economy in terms of observing time, but it makes an accurate calibration problematic.

The data reduction have been performed by means of the UVES Pipeline in the MIDAS echelle context. The wavelength calibration has been performed using the new atlas of ThAr spectrum by Lovis & Pepe (2007), which increases the laboratory wavelength precision by means of HARPS observations, with the line selection suggested by Murphy et al. (2007) to avoid blends. Mean residuals of $\leq 0.37 \text{ mÅ}$ for the blue arm, $\leq 0.46 \text{ mÅ}$ for the red low and $\leq 0.55 \text{ mÅ}$ for the red up are generally obtained providing a velocity accuracy at the central wavelengths of $\leq 25 \text{ m s}^{-1}$ in the red and of $\leq 30 \text{ m s}^{-1}$ in the blue as shown in detail in Fig. 1. We note that these residuals are about one order of magnitude smaller than those derived by Chand et al. (2006). They can be further improved for limited portions of the spectrum where the reduction is optimized as achieved by Levshakov et al. (2007). As shown by de Cuyper & Hensberge (1998) an accuracy of 10^{-2} of the pixel, which in UVES is $\approx 15 \text{ m s}^{-1}$, is attainable for non blended ThAr lines with more than 10^3 detected electrons in the central pixels. However, the accuracy of the ThAr lines themselves is of the order of 10 to 100 m s^{-1} and this is not directly reflected in the residuals of the wavelength calibration. The reduced spectra have been normalized manually tracing the continuum by means of the standard MIDAS routine.

For the reduction of the twilight spectra we skipped the automatic sky subtraction and extracted the spectra from the calibrated frames manually by using the standard MIDAS echelle commands, using a slit height of 8 pixels to minimize effects due to the small curvature of the slit projection on the detector. To check the curvature effects we extracted 2 spectra from the same image with an extraction slit of 2 pixels and offset by 3 pixels above and below the central position of the order. The position of spectral lines on the two extracted spectra did not reveal notable shifts due to curvature effects.

The angular sizes of the two asteroids in the epoch of observations were of 0.278 arcsec and 0.263 arcsec, and always smaller than the night seeing. They are effective point sources and the light follows the same path through the atmosphere, telescope and spectrograph not differently from a QSO or other point-like sources. Thus with asteroid observations the radial velocity accuracy could be monitored along the echelle orders for the whole frame in a much better way than with the calibration lamp since the asteroid lightpath takes into account the atmospheric variations and the centering of the object on the slit. In particular, in the case of UVES observations which make use of the dichroic we can monitor the response of the two separate arms. In the twilight spectrum the diffuse day-light illuminates the slit uniformly so that a comparison between the radial velocity of the asteroid and the day-light probes slit illumination effects on radial velocities.

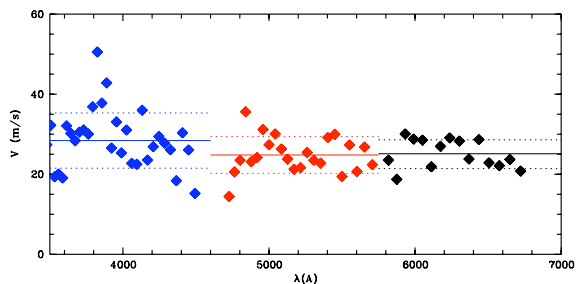
UVES is also equipped with an iodine absorption cell which can be inserted in the beam to obtain a dense grid of iodine absorption lines superimposed on the target spectrum. The iodine cell currently mounted on UVES produces a rich absorp-

Table 1. Journal of asteroid observations and basic data. Ceres spectra has been observed by HARPS. Expected radial velocities and its components are given in columns 6, 7 and 8. For Ceres the values refer to mid exposure.

Name	Date	JD	V mag	exp. sec	$RV_{ast-par}$ km s ⁻¹	$RV_{ast-\odot}$ km s ⁻¹	ΔRV km s ⁻¹
Iris	18/12/06	2454088.518086	7.83	300	12.707	1.704	14.411
	22/12/06	2454092.514539	7.95	300	13.777	1.830	15.607
	23/12/06	2454093.514000	7.98	300	14.030	1.862	15.892
	24/12/06	2454094.515400	8.01	300	14.283	1.893	16.176
	25/12/06	2454095.513566	8.04	450	14.521	1.924	16.445
Juno	24/01/07	2454125.880451	10.62	600	-21.403	3.731	-17.672
	25/01/07	2454126.873002	10.61	900	-21.364	3.721	-17.643
	29/01/07	2454130.873891	10.57	900	-21.065	3.683	-17.382
	31/01/07	2454132.846757	10.55	900	-20.949	3.664	-17.285
Ceres	15/07/06	2453932.837256	8.00	1800	-11.288	0.456	-10.832
	22/05/06	2453877.919808	8.85	900	-22.707	0.690	-22.017

Table 2. Sky observations and data, *spectra taken with HARPS

Date	JD	$RV_{par-\odot}$ km s ⁻¹
18/12/06	2454088.480700	0.238
22/12/06	2454092.481400	0.263
23/12/06	2454093.479390	0.272
24/12/06	2454094.478500	0.279
25/12/06	2454095.480300	0.286
25/01/07	2454126.472293	0.573
31/01/07	2454132.482003	0.629
14/07/06*	2453931.425152	0.302
22/10/05*	2453666.426383	-0.070

**Fig. 1.** Typical order residuals of the wavelength calibration, namely the difference between the measured and laboratory wavelength of the ThAr lines used in the calibration. The plotted ones are for Iris 22 Dec 2006. The three groups, with mean values and 1σ dispersion over plotted, refer to the 3 CCDs which have been reduced independently.

tion line spectrum in the range 490–640 nm. Butler et al. (2004) achieved an accuracy of 0.42 m s^{-1} for UVES with observations of α Cen A by means of a series of 3013 spectra of 1–3 s exposures, but after correcting for trends and jumps. However, iodine cell is not well suited for measuring accurate positions of QSO absorption lines which fall very far apart, and we are not aware of its use for this purpose.

3. Asteroids as radial velocity standards

Out of 111 stars observed in 20 years with the two CORAVEL spectrometers only a minor fraction shows variability of $\approx 200 \text{ m s}^{-1}$ (Udry et al. 1999). Thus radial velocity standard stars provide a reference system of radial velocities with a precision of several hundred m s^{-1} . Among the celestial sources the asteroids are probably the best radial velocity standard sources and at least for two reasons. The former is that they reflect sunlight without any modification of the solar spectrum and the latter is that their velocity component with respect to the observer can be predicted with very high accuracy reaching the m s^{-1} level (Zwitter et al. 2007).

The first condition is strictly valid only for relatively large asteroids with a nearly spherical shape which produce a constant reflectance of the sunlight. The two selected asteroids Iris and Juno have radii of 99.9 and 117.0 km respectively and a spherical shape. On the 18 Dec observation of Iris the illuminated fraction were of 97.07% and on the 24 Jan 2007 Juno had a 97.26 % reflectance so that the reflected and the direct solar spectra are likely identical. Variation of reflectance with wavelength or presence of regolith developed by meteoroid impact on the asteroid do not affect high resolution spectra. Also the asteroid rotation does not affect the solar spectrum and is much smaller than the solar one. The rotational periods for Iris and Juno are of 7.14 and 7.21 hours respectively. Thus their rotational velocity would be of about 25 m s^{-1} , which is much lower than the solar one and it will not cause further significant broadening.

The second reason is that the component of their motion relative to the observer on the earth can be calculated with extreme accuracy. For asteroids with radar monitoring, the orbital computations can take into account the interferences of other bodies of the solar system including the major asteroids and reach precisions at the level of the m s^{-1} (Zwitter et al. 2007).

Table 1 reports the motion components and the resulting expected radial velocity shifts ΔRV . Ephemeris for our objects has been computed by means of the JPL's Horizons system¹ which provides accurate ephemeris for the minor bodies of the solar system. The sunlight reflected by the asteroid is shifted by the heliocentric radial velocity of the asteroid with respect to the sun at the time t_1 when the photons left the asteroid and were shifted by the component of the earth rotation towards the asteroid at the time t_2 , when the photons reach the earth. The latter is the projection along the line-of-sight of the asteroid motion with respect to the observer at the Paranal site adjusted for aberration, and comprises both the radial velocity of the asteroid and the component due to the earth rotation towards the line of sight. At Paranal the observed asteroid radial velocity is

$$\Delta RV = (RV_{ast-par} + RV_{ast-\odot}) \quad (1)$$

We also take as reference several twilight spectra which are listed in Table 2. The radial velocity of the skylight reflected by the terrestrial atmosphere is also shifted by the heliocentric earth radial velocity. This component, $RV_{par-\odot}$, is given in the last column of Table 2. The precise position of the scattering of solar light by the atmosphere is not known but it should be within 10 km from the ground. In the next sections we will show that the scattered light from the atmosphere probably keeps the transversal motions of the atmosphere and therefore it is not possible to predict its velocity with the desired accuracy.

4. Asteroids with UVES

4.1. Solar absolute reference

The highest quality solar spectra in the optical domain are the FTS solar flux and disc-center atlas obtained at the McMath telescope at Kitt Peak by Kurucz et al. (1984) and Brault & Neckel (1987). These atlases achieve a signal-to-noise ratio of about 2500 with a resolving power of 400,000. Allende Prieto & Garcia Lopez (1998a,b) used these atlases to measure the central wavelength for a considerable number of lines. Gravitational shifts and convective motions are responsible of line to line displacements which can be of several hundreds of $m s^{-1}$. These displacements vary with the solar cycle showing a modulation with a peak to peak variation of $30 m s^{-1}$ on the 11 years solar activity period with the positions more redshifted in correspondence of the maximum of activity (Deming & Plymate 1994). However, McMillan et al. (1993) did not reveal any drift within $4 m s^{-1}$ in the solar line position from a long data series spanning the period from 1987 to 1992. Allende Prieto & Garcia Lopez (1998a,b) line positions have a precision of the order of ≈ 50 – $150 m s^{-1}$ so that they provide absolute reference at this level. The lines formed at the top of the photosphere show shifts close to the gravitational redshift of $636 m s^{-1}$ while the other lines show the effects of convective motions with variable blue shifts of several hundreds of $m s^{-1}$. Lines with equivalent width stronger than $200 m\text{\AA}$ are rather insensitive to the convective shifts and have been used to estimate the absolute zero of the scale. The value at the plateau level is of $612 \pm 58 m s^{-1}$ in the case of the solar atlas of Kurucz et al. (1984) which shows the results closest to the theoretical gravitational shift.

We thus compare the measured line positions of the asteroid spectra with the solar line positions provided by Allende Prieto & Garcia Lopez (1998a) for the solar atlas of Kurucz et al. (1984). In fact the sun light reflected by the asteroids is a

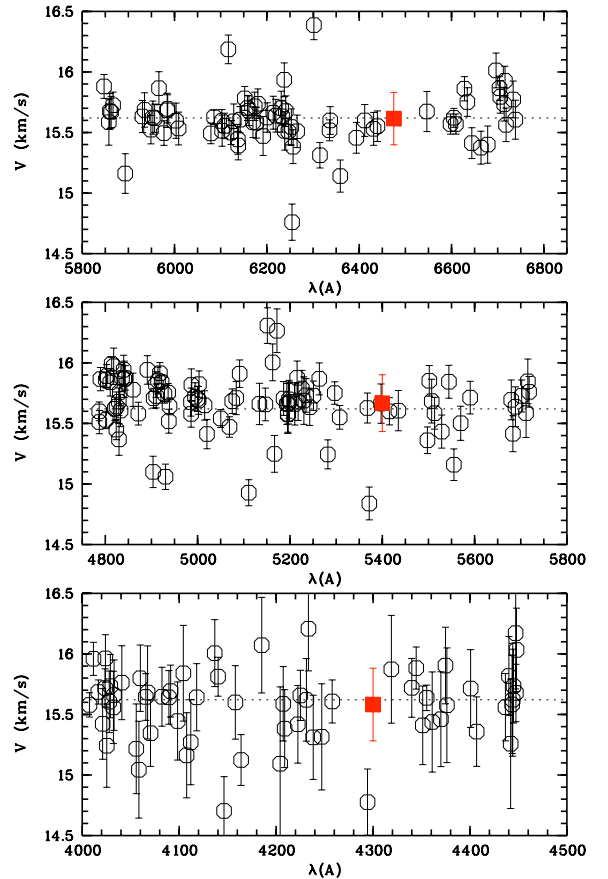


Fig. 2. Line shifts of Iris 23 Dec 2006 with reference of the Allende Prieto & Garcia Lopez (1998a) solar line wavelengths, see text for details. The dotted line shows the expected velocity of the asteroid. The top panel refer to the red-up CCD, the middle panel to the red-low CCD, and the bottom panel the blue CCD. The mean values and their dispersion are shown with the squares in the middle of each panel.

sort of integrated solar flux as the Kurucz et al. (1984) atlases. Fig. 2 shows the ΔRV measures for the Iris spectrum of 23 Dec 2006. The figure shows that there are no major wavelength calibration inaccuracies at the level of $200 m s^{-1}$ which corresponds to about 0.1 of the pixels size. The result shows a mean value of $\Delta RV = 15.614 \pm 0.203 km s^{-1}$ for the 75 lines measured in the red-up CCD, a $\Delta RV = 15.668 \pm 0.234 km s^{-1}$ for 96 lines in the red-low CCD, and of $15.582 \pm 0.300 km s^{-1}$ for 63 lines in the blue CCD. Considering that the expected velocity is of $\Delta RV = 15.620 km s^{-1}$, there is an excellent agreement with the red-up CCD and a slight offset of about $50 m s^{-1}$ and $30 m s^{-1}$ with the red-low and blue CCD respectively. Despite the scatter of ≈ 200 – $300 m s^{-1}$, this analysis shows that there is no significant offset between the two arms of UVES implying that there is no mis-centroiding of the target on the two slits of UVES arms.

4.2. Asteroid versus asteroid

To overcome the intrinsic uncertainties in the positions of the solar lines we compare the solar spectrum from an asteroid taken in two different epochs. In this way each line is compared with itself leaving only the instrumental and calibration imprinting

¹ Available at <http://ssd.jpl.nasa.gov/horizons.cgi>

on the change of the asteroid radial velocity between the two epochs.

To measure accurately the radial velocity difference between two lines we have implemented and adapted a procedure from Levshakov et al. (2006). The most probable ΔRV between two lines is found by varying ΔRV by small incremental steps and estimating the χ^2 of the fit. Fig. 3 shows a portion of the red-low frame of Juno 31 Jan and of the sky spectrum of the same day around line 5217.09 Å. The S/N are of 126 and 295 for Juno and twilight, respectively calculated from two nearby continuum windows bracketing the line position. The range used in the fitting is marked by thick curves on the upper panel of the figure and we consider only the central parts of the absorption lines to avoid the influence of the wings.

From the fit of points in the vicinity of the global χ^2_{\min} the procedure computes a parabola with the radial velocity difference as variable. The 1σ uncertainty interval is then calculated from the parabola when $\chi^2(\Delta v) - \chi^2_{\min} = 1$. For this particular case we have obtained $\Delta RV = -17.723 \pm 0.033 \text{ km s}^{-1}$ at 1σ .

The error is rather typical of our measurements and corresponds to about 0.02 of the pixel size. For instance, in computing the difference between the Iris spectra taken on 18 and 22 Dec 2006, the 203 lines measured have a mean error of $39 \pm 3 \text{ m s}^{-1}$, and of $37 \pm 2 \text{ m s}^{-1}$, respectively. The error is mainly the photon noise error and it depends from the signal to noise ratio of the two spectra. This error sets the precision of our analysis and the level of instrumental effects which can be recovered. In principle with higher signal-to-noise spectra this level can be further improved. Wavelength calibration errors are not expected to contribute very much to this error because even if the wavelength calibrations of two spectra are performed independently, they likely make use of the same Ar or Th lines in deriving the calibration coefficients.

The results of the radial velocity difference between the Iris spectra taken on 18 with those of 22 and 23 Dec 2006 are shown in Figs. 4 and 5. The measures are performed on lines falling onto 7 orders for each CCD frame selected to map the full spectral range. On the right side of each panel the average value for each single order is reported with the sample standard deviation. As it can be seen from the top panel of the figure, the measurements do not show evidence for trends within an individual order, and the measures are normally distributed around their mean value. At the bottom of the figure the mean values for each order are plotted as a function of the order number. There is no evidence of any pattern of the measured radial velocity with wavelength from 3500 Å up 6750 Å with measurements involving 3 CCDs and two spectrograph arms. For the 18-22 comparison the mean of the 3 CCDs are $\Delta RV = 1.157 \pm 0.073 \text{ km s}^{-1}$ for the blue, $1.140 \pm 0.048 \text{ km s}^{-1}$ for the red-low and $1.134 \pm 0.048 \text{ km s}^{-1}$ for the red-up. The excess in the dispersion observed within each order reflects the combined contribution of wavelength calibration and data reduction errors with the statistical error. The mean of the mosaic of the two CCDs of the red arm is only 19 m s^{-1} away from the value of the blue arm. For the comparison between 18 and 23 Dec observations we have a mean value for the blue CCD of $1.487 \pm 0.042 \text{ km s}^{-1}$ and for the mean of the two red CCDs a value of $1.464 \pm 0.036 \text{ km s}^{-1}$, or 23 m s^{-1} away from the blue arm.

Therefore, there is no evidence for a significant misalignment between the two arms of the UVES spectrograph. However, the expected radial velocity difference between the two epochs in which the asteroid was observed is of 1.190 km s^{-1} and of 1.447 km s^{-1} , respectively. Taking the mean

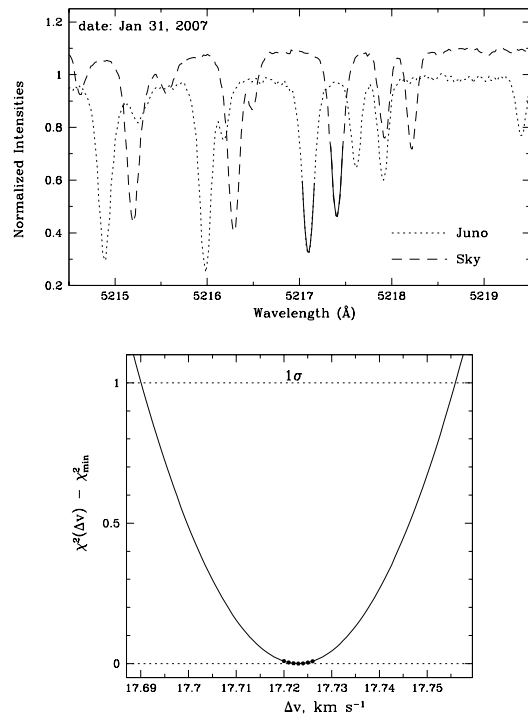


Fig. 3. Procedure for the determination of an accurate ΔRV and its error. On the top panel the normalized sky spectrum is slightly shifted vertically for display purposes.

value of the two arms we miss the expected velocity by 43 and 24 m s^{-1} in the two comparisons. This implies a sort of systematic error in one or in all the observations. The origin of this systematic error is likely to be ascribed to a non-uniform illumination of the slit.

Given that there is no evidence for a systematic behavior within the orders in the rest of our observations we have performed a cross-correlation to get order shifts by means of the IRAF-rvsao XCSAO routine. For this kind of analysis particular care has been adopted in selecting spectral regions without telluric lines which perturb the cross correlation. At the bottom of Figs. 4 and 5 the measures based on single lines, plotted in dots, with those performed by means of the XCSAO, plotted in diamonds, are showing that the two procedures are providing consistent results. The results are reported in Table 3 and summarized in Table 4. These measurements performed on the whole set of observations at our disposal confirm that there are not notable patterns with wavelength, no offsets between the two UVES arms and that offsets with respect to the expected velocity in the range $10\text{--}50 \text{ m s}^{-1}$ are common.

5. Asteroids with HARPS

To check the whole procedure by means of a different instrument specifically designed for high precision radial velocity studies, we retrieved two reduced spectra of Ceres from the public HARPS archive and applied the same kind of measures performed with UVES. The High Accuracy Radial velocity Planet Searcher at the ESO La Silla 3.6m telescope is a spectrograph dedicated to the discovery of extrasolar planets through radial velocity oscillations. It is a fibre-fed high resolution echelle spectrograph and is contained in a vacuum vessel to avoid spectral drift due to temperature and air pressure variations. There

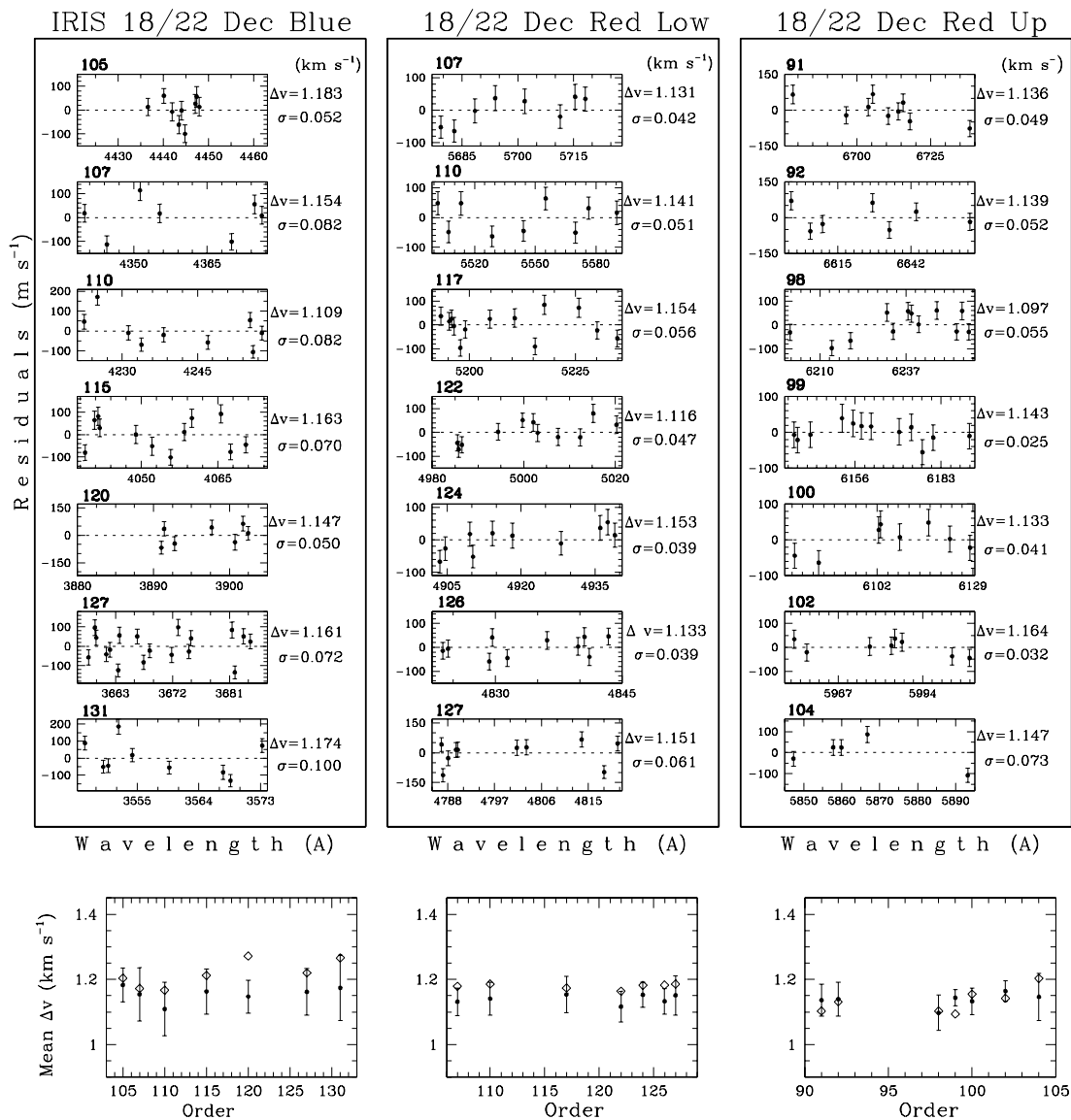


Fig. 4. Radial velocity difference from Iris 18 and 22 Dec 2006. Residuals correspond to the difference Iris(22) – Iris(18). The predicted ΔRV is 1.190 km s^{-1} . Individual echelle orders (numbered by bold) are shown in the upper panels. For each order the mean value Δv and the sample standard deviation σ are indicated. These values Δv and σ are also shown by dots with error bars in the corresponding low panels where results obtained through the cross-correlation analysis (diamonds) are plotted for comparison.

are two fibers, one collects the star light, while the second is used to record simultaneously a ThAr reference spectrum. Both fibres are equipped with an image scrambler to provide a uniform spectrograph pupil illumination, independent of pointing decentering. In this way the instrument is able to obtain a long term radial velocity accuracy of the order of 1 m s^{-1} for the entire optical spectrum of a slow rotating G type star or cooler (Pepe et al. 2005). HARPS has a resolving power of $R \approx 120,000$ and provides a sampling of the slit of $\text{FWHM} = 4.1$ pixels of 15μ size. Due to the relatively smaller size of the telescope the exposures are rather long, being namely of 1800 s and 900 s (see Table 1). In the course of the exposure the radial velocity of the asteroid changes by ≈ 50 and 25 m s^{-1} respectively. The expected velocities reported in Table 1 refer to the mid exposure times.

In Fig. 6 the radial velocities measured between the observations of Ceres taken on 22 May 2006 and on 15 July 2006 are given. The accuracy of the measure of a pair shift is now better than $\approx 20 \text{ m s}^{-1}$ and the line to line variation of the positions is almost entirely due to errors in the wavelength calibration. The mean of the blue CCD Linda is $\Delta RV = 3.072 \pm 0.010 \text{ m s}^{-1}$, and the mean of the red CCD Jasmin is $3.080 \pm 0.010 \text{ m s}^{-1}$. The predicted ΔRV shift is of 3.070 km s^{-1} and is found in excellent agreement with the measured velocity within few m s^{-1} . This is highly suggestive that the systematic offset observed in the UVES spectra is related to the slit acquisition mode which remains the most significant observational and technical difference between the two spectrographs.

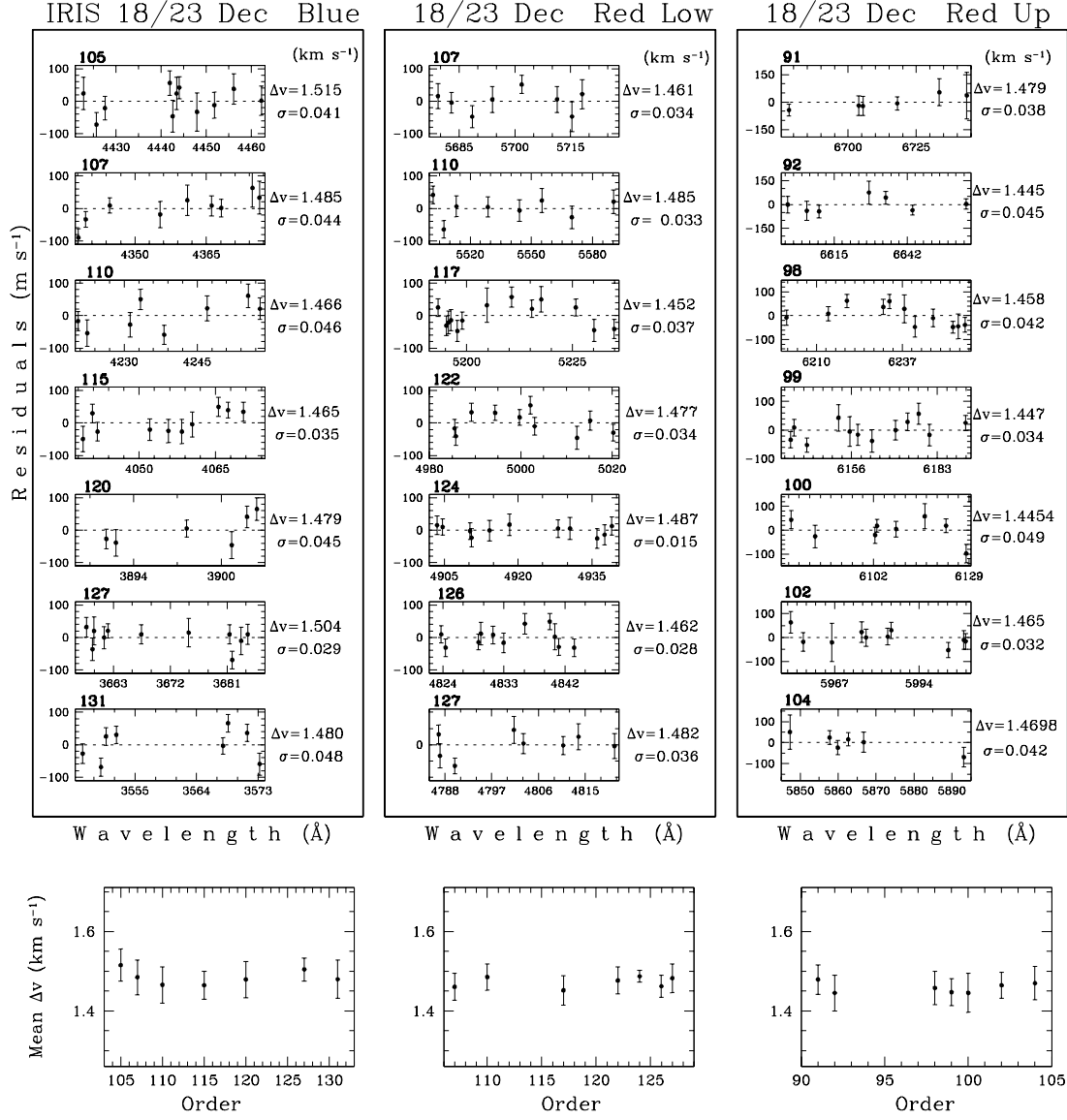


Fig. 5. Same as Fig. 4 but for the comparison between Iris 18 and 23 Dec 2006. The predicted ΔRV is 1.447 km s^{-1} . Residuals correspond to the difference Iris(23) – Iris(18).

6. Twilight

Sky observations differ from point source observations mainly because the slit is uniformly illuminated. Thus in principle a differential measure of a point-like source as an asteroid with the same feature from the sky spectrum allows us to probe radial velocity drifts induced by a non uniform slit illumination. The results of the measures for the Juno observations of 31 Jan are shown in Fig. 7. The observations of Juno on 31 Jan when compared with the skylight on 31 Jan show that the ΔRV inferred from the three CCDs are all consistent with each other. The blue CCD gives a mean value of $\Delta RV = -17.797 \pm 0.064 \text{ km s}^{-1}$, the red-low a $\Delta RV = -17.757 \pm 0.050 \text{ km s}^{-1}$, and the red-up a $\Delta RV = -17.772 \pm 0.057 \text{ km s}^{-1}$. The expected velocity is of $\Delta RV = -17.914 \text{ km s}^{-1}$, therefore we observed an offset of $\approx 150 \text{ m s}^{-1}$. This offset is rather high and about a factor three higher than that observed in the series of asteroid-asteroid comparison. To check the procedure we performed two separate tests. In one

test we compare the accurate HARPS observations of Ceres with a sky spectrum taken with the same instrument, and in a second test we compare two twilight spectra taken with UVES in two different epochs.

Fig. 8 shows the comparison between the spectrum of Ceres taken on 15 July 2006 with a sky light taken with the same instrument on 22 Oct 2005. The mean ΔRV values in the two HARPS CCDs are $\Delta RV = 23.657 \text{ km s}^{-1}$ for the blue CCD Linda, and $\Delta RV = 23.647 \text{ km s}^{-1}$ for the red CCD Jasmin, while the predicted one is of $\Delta RV = 23.709 \text{ km s}^{-1}$ computed for the middle Ceres's exposure. This measure shows an offset of $\approx 50 \text{ m s}^{-1}$ between the Ceres and sky spectrum. This offset is not observed when the Ceres of two epochs are compared with each other, as we discussed in the previous section. HARPS is fed by fiber optics and therefore no difference is expected between the two kind of measures suggesting that the sky spectrum holds a component of motion of several tens of m s^{-1} . This implies that the twilight

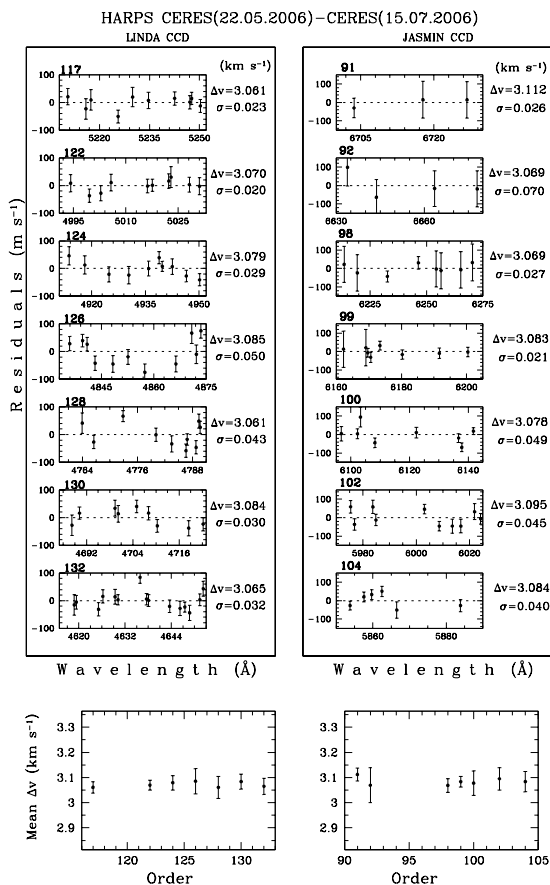


Fig. 6. ΔRV between Ceres 22 May and 15 July 2006 . The expected ΔRV is 3.070 km s^{-1}

solar spectrum is not a good reference for the determination of the zero scale.

As a second test we compared the sky spectra with each other. The difference between the sky spectra taken with HARPS on 22 May 2005 and 14 July 2006 are shown in Fig. 9. The expected velocity difference for this pair is of -371 m s^{-1} while the mean value is $-275 \pm 39 \text{ m s}^{-1}$. Thus, also in this case we fail to reproduce the expected velocity confirming that the sky spectrum is sensitive to unpredictable motions likely due to currents in the upper terrestrial atmosphere.

We also emphasize that close inspection of UVES twilight and asteroid solar spectra show that they are not completely identical. Small differences at the level of 1-2% are found between the twilight spectrum and the asteroid reflected solar spectrum consistently with what found by Zwitter et al. (2007). An example of the two spectra, with the skylight lines shallower, is shown in Fig. 10. Similar differences have been found also by Gray et al. (2000) and also depending on the angular separation from the Sun. According to Gray et al. (2000) the skylight variations can be explained as a combination of Rayleigh-Brillouin scattering with a second term of aerosol. The measure of the FWHM for a representative sample of lines from asteroid spectra and for twilight are shown in Fig. 11. The FWHM of the twilight are significantly larger by about 5 mÅ with comparison to the asteroid lines. The broader twilight lines suggest the presence of turbulence in the atmospheric motions which reflect the sun light. At twilight a transverse motion in the atmosphere has a considerable component in the direction of the sun which is low

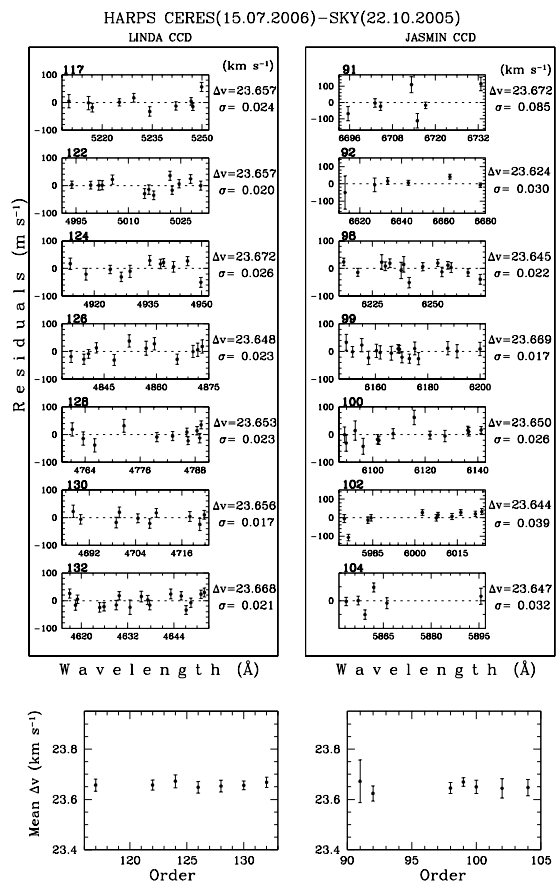


Fig. 8. ΔRV between Ceres 15 July 2006 and the Sky on 22 Oct 2005 . The predicted ΔRV is 23.709 km s^{-1} .

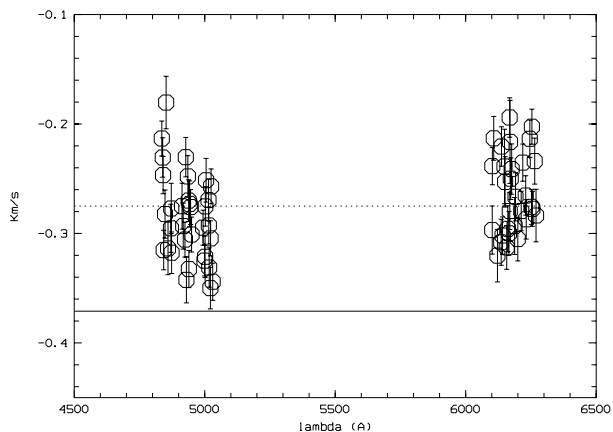


Fig. 9. ΔRV between HARPS sky of 22 May 2005 and 14 July 2006. The dotted line is the mean value while the red line shows the expected ΔRV at -371 m s^{-1} .

above the horizon when the observations were made and produce a radial velocity drift when observed in the reflected spectrum. A detailed investigation of these effects is beyond the scope of this paper, but the presence of these effects shows that the twilight spectrum is not a good zero reference point at the level of $\approx 100 \text{ m s}^{-1}$.

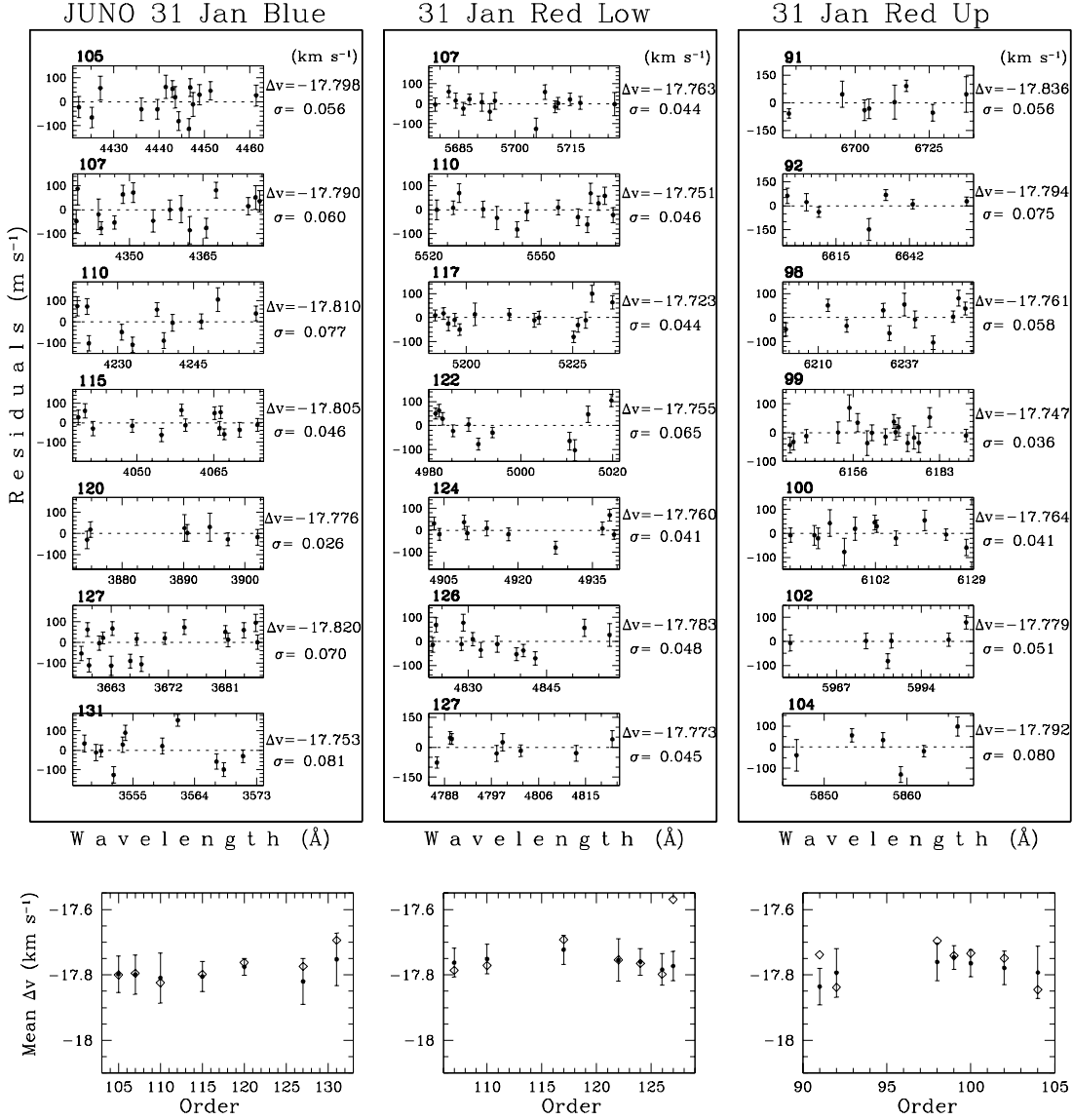


Fig. 7. Juno 31 January relatively to the twilight of the same date. Residuals correspond to the difference Juno – Sky.

7. Implications for $\Delta\alpha/\alpha$

In the Many Multiplet method the measurability of $\Delta\alpha/\alpha$ from observations of absorption lines in QSO spectra is based on the fact that the energy of each line transition shows a different sensitivity on a change of α (Webb et al. 1999). Thus, the value of $\Delta\alpha/\alpha$ depends on the measure of the relative radial velocity shifts, ΔRV , between lines with different sensitivity coefficients. The relation between the radial velocities and $\Delta\alpha/\alpha$ is (Levshakov et al. 2006):

$$(v_2 - v_1) = 2c(Q_1 - Q_2) \frac{\Delta\alpha}{\alpha}, \quad (2)$$

where Q is the sensitivity coefficient $Q = q/\omega_0$, with ω_0 being the frequency and q the theoretical so-called q-factor. The q-factors have been computed for the most important UV resonance transitions by Dzuba et al. (2002) and for Fe II were recalculated by Porsev et al. (2007).

The largest ΔQ is presently provided by the Fe II resonance lines. By comparing the Fe II $\lambda 1608$ with and Fe II $\lambda 2382$ or

$\lambda 2600$ lines ($Q_{1608} = -0.0166$, $Q_{2382} = 0.0369$, and $Q_{2600} = 0.0367$ from Porsev et al. 2007) we obtain $|\Delta Q| \approx 0.053$ which is almost two times larger than that obtained from a combination of other transitions. In this case a shift of $\approx 30 \text{ m s}^{-1}$ between the Fe II lines corresponds to a $\Delta\alpha/\alpha$ of $\approx 1 \text{ ppm}$.

Levshakov et al. (2007) analyzed Fe II profiles associated with the $z_{\text{abs}} = 1.84$ Damped Ly α system from UVES observations of the quasar Q 1101–264. The data represent one of very few spectra of QSOs obtained with spectral resolution FWHM of 3.8 km s^{-1} and $S/N > 100$. In this work a shift of the relative radial velocity between the $\lambda 1608$ and $\lambda 2382$, 2600 lines of $\Delta RV = -180 \pm 85 \text{ m s}^{-1}$ was obtained. With the updated sensitivity coefficients from Porsev et al. (2007) this shift in the radial velocity between the Fe II lines corresponds to a $\Delta\alpha/\alpha = 5.66 \pm 2.67 \text{ ppm}$.

The Fe II lines fall at $\lambda \sim 4566 \text{ \AA}$ and $\lambda \sim 6765, 7384 \text{ \AA}$, respectively, quite far apart in the two different UVES arms so that a hidden systematic effect would challenge the interpretation as due to variation of α . Levshakov et al. (2007) measured the

Table 3. Cross correlation analysis: differential radial velocity shifts measured in km s^{-1} with respect of Iris 18 Dec 2006. The first column reports the echelle orders for the three chips blue, red-low and red-up. Xcsao σ are also indicated.

Iris B	range Å	18-22/12		18-23/12		18-24/12		18-25/12	
		km s ⁻¹	σ	km s ⁻¹	σ	km s ⁻¹	σ	km s ⁻¹	σ
105	4420.7 - 4463.0	-1.204	0.027	-1.447	0.008	-1.704	0.010	-2.091	0.009
107	4338.5 - 4379.2	-1.172	0.046	-1.450	0.008	-1.706	0.010	-2.085	0.009
110	4220.7 - 4259.2	-1.167	0.028	-1.441	0.006	-1.776	0.008	-2.070	0.007
115	4038.0 - 4073.3	-1.212	0.018	-1.438	0.007	-1.764	0.009	-2.055	0.010
120	3888.0 - 3902.8	-1.272	0.030	-1.476	0.012	-1.761	0.012	-2.051	0.011
127	3650.0 - 3686.9	-1.220	0.025	-1.501	0.012	-1.715	0.024	-1.999	0.014
131	3540.0 - 3573.9	-1.266	0.055	-1.498	0.060	-1.643	0.071	-2.036	0.063
RL									
107	5675.2 - 5728.5	-1.179	0.029	-1.462	0.007	-1.705	0.011	-2.095	0.008
110	5521.1 - 5571.6	-1.186	0.025	-1.452	0.009	-1.774	0.013	-2.097	0.009
117	5192.2 - 5236.8	-1.174	0.021	-1.403	0.007	-1.763	0.011	-2.071	0.012
122	4981.0 - 5005.0	-1.157	0.008	-1.465	0.006	-1.717	0.008	-2.103	0.007
124	4900.3 - 4923.3	-1.167	0.009	-1.468	0.007	-1.749	0.009	-2.102	0.009
126	4822.8 - 4845.0	-1.183	0.041	-1.461	0.008	-1.726	0.011	-2.084	0.009
127	4810.0 - 4822.8	-1.190	0.027	-1.470	0.013	-1.752	0.043	-2.117	0.018
127	4786.4 - 4805.0	-1.183	0.024	-1.436	0.012	-1.740	0.020	-2.135	0.026
RU									
91	6667.5 - 6741.2	-1.103	0.047	-1.442	0.024	-1.701	0.042	-2.145	0.038
92	6595.5 - 6667.6	-1.131	0.026	-1.461	0.031	-1.773	0.032	-2.181	0.030
98	6193.7 - 6257.3	-1.103	0.012	-1.463	0.011	-1.777	0.014	-2.120	0.012
99	6131.5 - 6193.7	-1.094	0.011	-1.456	0.009	-1.774	0.010	-2.098	0.009
100	6077.0 - 6131.5	-1.155	0.015	-1.431	0.011	-1.689	0.016	-2.105	0.018
102	5995.0 - 6010.7	-1.142	0.017	-1.452	0.022	-1.741	0.027	-2.144	0.027
104	5841.0 - 5885.0	-1.203	0.036	-1.487	0.021	-1.659	0.019	-2.065	0.020
Juno									
B	range Å	18-24/01		18-25/01		18-29/01		18-31/01	
		km s ⁻¹	σ	km s ⁻¹	σ	km s ⁻¹	σ	km s ⁻¹	σ
105	4420.7 - 4463.0	32.203	0.035	32.058	0.031	31.849	0.031	31.706	0.033
107	4338.5 - 4379.2	32.282	0.034	32.067	0.030	31.787	0.030	31.657	0.030
110	4220.7 - 4259.2	32.249	0.051	32.044	0.049	31.839	0.051	31.648	0.050
115	4038.0 - 4073.3	32.224	0.035	32.034	0.032	31.792	0.092	31.709	0.033
120	3888.0 - 3902.8	32.136	0.067	32.026	0.067	31.848	0.066	31.674	0.070
127	3650.0 - 3686.9	32.183	0.041	32.090	0.041	31.859	0.046	31.656	0.049
131	3540.0 - 3573.9	32.154	0.082	32.050	0.077	31.783	0.087	31.623	0.074
RL									
107	5675.2 - 5728.5	32.157	0.032	32.046	0.033	31.742	0.029	31.614	0.028
110	5521.1 - 5571.6	32.112	0.049	32.022	0.048	31.794	0.046	31.584	0.047
117	5192.2 - 5236.8	32.086	0.037	31.995	0.034	31.789	0.038	31.577	0.037
122	4980.3 - 5021.3	32.129	0.042	32.078	0.045	31.705	0.036	31.567	0.037
124	4900.3 - 4940.0	32.137	0.102	31.898	0.068	31.690	0.074	31.558	0.105
126	4822.8 - 4845.0	32.123	0.106	32.013	0.101	31.739	0.103	31.648	0.105
127	4810.0 - 4822.8	32.002	0.160	31.832	0.157	31.652	0.149	31.415	0.137
127	4785.0 - 4805.0	32.064	0.113	31.985	0.046	31.716	0.099	31.579	0.111
RU									
91	6667.5 - 6741.2	32.209	0.118	32.059	0.097	31.765	0.109	31.558	0.075
92	6595.5 - 6667.6	32.134	0.110	31.932	0.098	31.698	0.083	31.481	0.073
98	6193.7 - 6257.3	32.109	0.040	32.012	0.041	31.809	0.036	31.658	0.035
99	6131.5 - 6193.7	32.112	0.045	32.020	0.041	31.795	0.038	31.630	0.038
100	6077.0 - 6131.5	32.197	0.063	32.051	0.059	31.824	0.052	31.589	0.050
102	5995.0 - 6010.7	32.184	0.049	31.978	0.042	31.741	0.048	31.610	0.037
104	5841.0 - 5885.0	32.172	0.064	32.087	0.064	31.721	0.063	31.601	0.063

same velocity between the $\lambda 2382$ and $\lambda 2600$ which is what expected since the Q values for $\lambda 2382$ and $\lambda 2600$ are about equal. However, there is no direct way to check out systematic differences of the Fe II $\lambda 1608$ with lines that fall in the other arm of the spectrograph. Different velocity offsets may occur in the blue

and red frames causing an artificial Doppler shift between the Fe II $\lambda 1608$ and $\lambda \lambda 2382, 2600$ lines and mimicking a change in $\Delta\alpha/\alpha$. The set of measures carried out here show that there are no ΔRV offsets between the two UVES arms greater than 30 m s^{-1} . This excludes this kind of systematics as a possible ori-

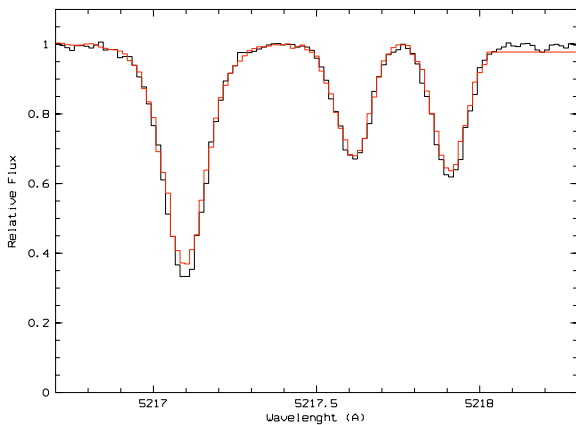


Fig. 10. Portion of the asteroid (thick line histogram) and twilight (thin line histogram) spectrum around the line 5217.3 Å.

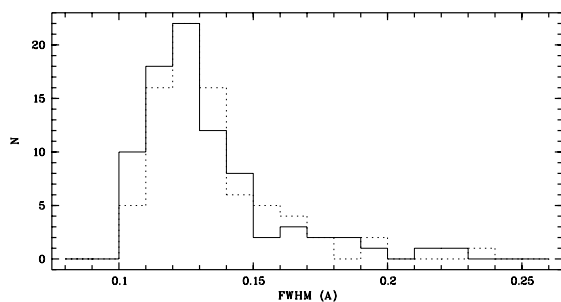


Fig. 11. FWHM for asteroid Juno (solid line) and twilight (dashed line).

gin of the signal detected by Levshakov et al. (2007). Therefore, either the detection is real or it is induced by a systematic of different kind.

8. Conclusions

Observations of asteroids have been conducted with the UVES spectrograph at the VLT to probe the radial velocity accuracy achievable with the spectrograph. By means of HARPS observations we have shown that the asteroid observations are excellent radial velocity standards able to probe the instrumental accuracy in any particular position of the spectrum down to the limit provided by the ThAr wavelength calibration, or 10 m s^{-1} .

By comparing the asteroid line positions with the absolute ones from solar positions which account for solar convective shifts we have shown that the UVES spectrograph is not affected by any systematics along the whole optical domain at the level where the solar line positions are known, namely of few hundreds of m s^{-1} . We have further refined the analysis by comparing of asteroid in different epochs. No major distortions in the wavelength are found, namely not higher than about 30 m s^{-1} , where this limit is set by the photon noise of our observations. We do indeed reveal zero offsets in the range 0 up to $\approx 50 \text{ m s}^{-1}$. With reference to similar observations performed with HARPS we suggest that this is likely due to a non uniform slit illumination. Attempts to use the twilight spectra to quantify the drifts induced by non-uniform illumination shows instead that twilight

spectrum contains additional turbulence and motions, and therefore cannot be used as a reliable zero reference point.

The recorded spectrum does not show evidence of stretching of the wavelength scale or other instrumental effects in excess of the uncertainties induced by the wavelength calibration accuracy. In particular, the two UVES arms which are fed by two independent slits do not show signature for radial velocity offsets within the present accuracy of 30 m s^{-1} .

This result has important implications on the search for $\Delta\alpha/\alpha$ currently performed with UVES which relies on relative shifts of absorbing lines falling on rather distant spectral regions and sometimes belonging to different arms of the spectrograph. For instance, Levshakov et al. (2007) measure of a ΔRV difference of $-180 \pm 85 \text{ m s}^{-1}$ between Fe II transitions falling in the two different arms of UVES which provides evidence for a variation in the fine structure constant $\Delta\alpha/\alpha = 5.66 \pm 2.67 \text{ ppm}$. The present analysis shows that the line shift is unlikely produced by a misalignment of the the two slits at the entrance of the two UVES arms.

The proposed technique has a general validity and can be applied to any spectrograph to perform a real time quality control of the spectrograph performance during night time while the observations are carried on.

Acknowledgements. The asteroids observations were obtained in service mode in UVES calibration time. We are grateful to Cedric Ledoux and to all UVES operation astronomers for the careful job which has made possible these measurements. We thank also Fiorella Castelli and Cristophe Lovis for many useful discussions. Part of this work was supported by PRIN-INAF 2006. S.A.L. gratefully acknowledges the hospitality of ESO (Garching) and Osservatorio Astronomico di Trieste. This research has been supported by the RFBR grant No. 06-02-16489, by the Federal Agency for Science and Innovations grant NSh 9879.2006.2, and by the DFG project RE 353/48-1.

References

- Allende Prieto, C., & Garcia Lopez, R. J. 1998a, *A&AS*, 129, 41
- Allende Prieto, C., & Garcia Lopez, R. J. 1998b, *A&AS*, 131, 431
- Avelino, P. P., Martins, C. J. A. P., Nunes, N. J., & Olive, K. A. 2006, *Phys. Rev. D*, 74, 083508
- Brault, J., & Neckel, H. 1987, *Spectral Atlas of Solar Absolute Disk-Averaged and Disk-Center Intensity from 3290 to 12510*, unpublished. Tape-copy from KIS IDL library
- Butler, R. P., Bedding, T. R., Kjeldsen, H., et al. 2004 *ApJ*, 600, 75
- Copeland, E. J., Sami, M., & Tsujikawa, S. 2006, *Int. J. Mod. Phys.*, D15, 1753
- Chand, H., Srianand, R., Petitjean, P., & Aracil, B. 2004, *A&A*, 417, 853
- Chand, H., Srianand, R., Petitjean, P., Aracil, B., Quast, R., & Reimers, D. 2006, *A&A*, 451, 45
- de Cuyper, J.-P., & Hensberge, H. 1988, *A&AS*, 129, 409
- Deming, D., & Plymate, C. 1994, *ApJ*, 426, 382
- Dzuba, V. A., Flambaum, V. V., Kozlov, M. G., & Marchenko, M. V. 2002, *Phys. Rev. A*, 66, 022501
- Fujii, Y. 2007, arXiv:0709.2211
- Gray, D. F., Tycner, C., & Brown, K. 2000, *PASP*, 112, 328
- Kafer, A., D'Odorico, S., & Kaper, L. 2004, *UV-Visual Echelle Spectrograph. User Manual* (<http://www.eso.org/instruments/uves/userman/>), p. 40
- Kurucz, R. L., Furenlid, I. J., & Testerman, L. 1984, *NOAO Atlas No. 1, The Solar Flux Atlas from 296 to 1300 nm. Sunspot*, (NM: National Solar Observatory)
- Levshakov, S. A., Centurión, M., Molaro, P., & D'Odorico, S. 2005, *A&A*, 434, 827
- Levshakov, S. A., Centurión, M., Molaro, P., et al. 2006, *A&A*, 449, 879
- Levshakov, S. A., Molaro, P., Lopez, S., et al. 2007, *A&A*, 466, 1077
- Lovis, C., & Pepe F. 2007, *A&A*, 468, 1115
- Martins, C. J. A. P. 2006, arXiv: 0610665
- McMillan, R. S., Moore, T. L., Perry, M. L., & Smith, P.H. 1993, *ApJ*, 403, 801
- Murphy, M. T., Tzanavaris, P., Webb, J. K., & Lovis, C. 2007, *MNRAS*, 378, 221
- Murphy, M. T., Webb, J. K., & Flambaum V.V. 2006, arXiv: 0612407
- Murphy, M. T., Flambaum, V. V., Webb, J. K., et al. 2004, in *Astrophysics, Clocks and Fundamental Constants*, eds. S. G. Karshenboim and E. Peik (Springer-Verlag: Berlin, Heidelberg), p.131

Table 4. Summary of mean radial velocity shifts measured in km s⁻¹ with respect of Iris 18 Dec 2006.

Iris										
Date	ΔRV	Blue	σ	Red-low	σ	Red-up	σ	Red	Tot	σ
18-22/12	-1.196	-1.216	0.041	-1.179	0.011	-1.133	0.038	-1.156	-1.176	0.046
18-23/12	-1.481	-1.464	0.027	-1.474	0.063	-1.456	0.018	-1.465	-1.463	0.039
18-24/12	-1.765	-1.724	0.047	-1.750	0.039	-1.731	0.048	-1.740	-1.735	0.042
18-25/12	-2.034	-2.055	0.031	-2.092	0.015	-2.122	0.038	-2.107	-2.092	0.042
Juno										
Date	ΔRV	Blue	σ	Red-low	σ	Red-up	σ	Red	Tot	σ
18-24/01	32.083	32.204	0.051	32.101	0.050	32.160	0.041	32.130	32.152	0.063
18-25/01	32.054	32.053	0.021	31.983	0.087	32.020	0.052	32.002	32.017	0.063
18-29/01	31.793	31.822	0.033	31.730	0.052	31.765	0.047	31.747	31.770	0.058
18-31/01	31.696	31.668	0.031	31.568	0.068	31.590	0.057	31.579	31.606	0.068

- Pepe, F., Mayor, M., Queloz, D., et al. 2005, *The Messenger*, 120, 22
Porsev, S. G., Koshchev, K. V., Tupitsyn, I. I., Kozlov, M. G., Reimers, D., & Levshakov, S. A. 2007, *Phys. Rev. A*, 76, 52507
Quast, R., Reimers, D., & Levshakov, S. A. 2004, *A&A*, 415, L7
Srianand, S., Chand, H., Petitjean, P., & Aracil, B. 2007, arXiv: 0711.1742
Udry, S., Mayor, M., & Queloz, D. 1999, in *Precise Radial Velocities*, ed. J. B. Hearnshaw, & C. D. Scarfe, ASP Conf. Ser., 185, 367
Webb, J. K., Flambaum, V. V., Churchill, C. W., Drinkwater, M. J., & Barrow, J. D. 1999, *Phys. Rev. Lett.*, 82, 884
Zwitter, T., Mignard, F., & Crifo, F. 2007, *A&A*, 462, 795

List of Objects

‘Q 1101–264’ on page 9